Radiation Physics and Chemistry 95 (2014) 396–400

Contents lists available at ScienceDirect

Radiation Physics and Chemistry

journal homepage: www.elsevier.com/locate/radphyschem

# Gas–liquid distribution in a bubble column using industrial gamma-ray computed tomography

Carlos Henrique de Mesquita, Diego Vergaças de Sousa Carvalho, Rodrigo Kirita, Pablo Antonio S. Vasquez, Margarida Mizue Hamada*

*Instituto de Pesquisas Energéticas e Nucleares (IPEN/CNEN-SP), Av. Prof. Lineu Prestes, 2242, Cidade Universitaria, 05508-000 Sao Paulo, Brazil*

## HIGHLIGHTS

- An experimental bubble column was used to simulate an industrial distillation process.
- The bubble column was evaluated by gamma ray computed tomography technique.
- The holdup radial variation of the gas and liquid within the column was determined.
- A good spatial resolution was found for the developed third-generation tomography.
- The trend of bubble dispersion over the column was shown.

## ARTICLE INFO

*Article history:*
Received 28 September 2012
Accepted 14 February 2013
Available online 25 March 2013

*Keywords:*
Bubble column
Holdup
Multiphase systems
Industrial computed tomography
Phases distribution

## ABSTRACT

A gas absorption column used as a simulator bubble column for industrial processes was evaluated, using the third-generation industrial computed tomography developed at the IPEN. Gamma ray tomography experiments were carried out, using the simulator column empty and filled with water plus gas bubbling. The tomographic measurements were taken at three positions relative to the point of generation of the bubbles: above 20 mm, 120 mm and 320 mm. The resulting images describe the liquid or gas phase holdup distributions for bubbles generated in a hole of ∅=5 mm, located at 15 mm of the column wall. The developed third generation CT had a spatial resolution of 4.5 mm and a temporal resolution around 5 h/image. The trend of bubble dispersions, as they rise in the column, was shown.



## 1. Introduction

The gamma ray computed tomography (CT) technique for industrial processes evaluation has been indicated as the most promising to visualize the structure and the distribution of solids, liquids and gases inside multiphase systems. (Youssef et al., 2013; Kong et al., 2012; Youssef and Al-Dahhan, 2009; Al-Dahhan et al., 2007; Dudukovic, 2007; Hale et al., 2007; Johansen, 2005; Wu et al., 2001; Kumar and Dudukovic, 1997). The multiphase systems are structures that contain a mixture of solids, liquids and gases inside the chemical reactor or pipes in a dynamic process. These systems are widely used in many industries, for example, chemistry, food, pharmaceutical products and oil refinery (Youssef et al., 2013; Al-Dahhan et al., 2007; Dudukovic, 2007; Hale et al., 2007; Kantarcia et al., 2005). The gamma ray CT has been applied to visualize the distribution of churn-turbulent flow (Kantarcia et al., 2005) multiphase systems, giving to the analysts and engineers the conditions to obtain measurements in real time without interrupting the production. Among several applications, the CT has been used to improve the design, operation and troubleshooting of industrial processes (Kong et al., 2012; Youssef and Al-Dahhan, 2009; Al-Dahhan et al., 2007; Dudukovic, 2007; Hale et al., 2007; Johansen, 2005; Kumar and Dudukovic, 1997, Vasquez et al., 2010; Mesquita et al., 2010, 2011).

Scanners for transmission tomography employ radiation isotropic sources, such as an encapsulated gamma ray source, positioned in one side of the object to be scanned, and one or a set of collimated detectors arranged on the other side (Johansen, 2005; IAEA-TECDOC-1589, 2008). For industrial purposes there are basically four CT versions of scanners, among which the third and fourth generations are the most important and used nowadays. Briefly, the third-generation CT has better performance in spatial resolution while the fourth-generation CT has the best performance in the temporal resolution (Johansen, 2005; Mesquita et al., 2010, 2011). Usually, the analyzed objects in the industrial tomography field have high density and large dimensions,

* Corresponding author. Tel.: +55 11 3133 9779; fax: +55 11 3133 9765.
*E-mail addresses:* mmhamada@ipen.br, mmhamada@usp.br (M.M. Hamada).

0969-806X/$ - see front matter © 2013 Elsevier Ltd. All rights reserved.
http://dx.doi.org/10.1016/j.radphyschem.2013.02.028

requiring a high energy radiation source to across the material and a dense detector material to absorb the photons from the source (Calvo et al., 2009; Hubbell and Seltzer, 1996).

In this work, an experimental bubble column was used to simulate a churn-turbulent distillation process and tomographic measurements were taken at three positions relative to the point of bubble generation: above 20 mm, 120 mm and 320 mm, using a third-generation CT. A tomographic reconstruction algorithm (AM) (O'Sullivan and Benac, 2007) was used to calculate the spatial variation of the gas and liquid over the column cross section. The holdup radial variation of the gas and liquid within the column was also determined.

## 2. Experimental methods

A third generation computed tomography was developed for industrial applications at the CTR-IPEN (Mesquita et al., 2011). In its configuration, an array of five NaI(Tl) detectors of $5 \times 5$ cm$^2$ (diameter $\times$ thickness) were placed in a concentric arc opposite to the $^{137}$Cs (3.3 MBq) radioactive source and the detector-source system rotated around the centered target object. The five NaI(Tl) detectors are individually collimated with lead. Each collimator has a hole of $2 \times 5$ mm$^2$ (width $\times$ height) for beam sampling.

The target object is a gas absorption column (Armfield mod. UOP7), used as a simulator of churn-turbulent flow bubble column. It is a Perspex cylindrical tube of density $\delta \cong 1.2$ g/cm$^3$, $\varnothing_{int}=8$ cm internal diameter, $\varnothing_{ext}=9$ cm external diameter (0.5 cm wall thickness) and 140 cm height. The column comprises the following parts: liquid circuit (water), a gas circuit bubbled into a system containing a limiting hole of 0.5 cm located at 2.5 cm from the center of the column (1.5 cm from the column wall). The bubbles rise to the top of the column at a speed of about 300 cm/s. The tomographic measurements were firstly carried out using the empty column (filled with air) and after that with the column bubbled with water, i.e. the water is mixed and aerated by introduction of gas (5 l/min) into the bottom, forming the bubbles. For the bubble column, the tomographic measurements were taken at four positions relative to the point of bubble generation: above 5 cm, 10 cm, 20 cm and 30 cm (Fig. 1).

The system detector-collimator rotates around the column 47 times in arc of 0.79 deg/step, generating 47 projections per detector or a total of 235 projections ($=47$ steps $\times$ 5 detectors). Thereafter, the table containing the source and the detectors rotates 6° and this procedure is repeated until the table is rotated 360° ; totalizing 14100 ($=235 \times 360/6$) ray projections per image. The CT has temporal resolution about 5 h/image and spatial resolution of 4.5 mm. Therefore, the equipment has the ability to provide dynamic information only in average terms, that is, the CT may be capable of displaying the average of the absorption coefficient of the medium $\mu$(cm$^{-1}$) (water and gas), representing indirectly the density of the multiphase medium, which depends on the trend of the bubble path in the column.

The reconstruction algorithm used was the Alternative Minimization (AM) technique (O'Sullivan and Benac, 2007) implemented in FORTRAN and the data acquisition software was developed in Excel-VB.

## 3. Results and discussion

In columns containing two phases, gaseous and liquid, the reconstructed images generate the attenuation coefficients $\hat{\mu}_{g-l}(x,y)$ corresponding to the linear combination of the contribution of each phase, represented by Eq. (1).

$$\hat{\mu}_{g-l}(x,y) = \hat{\mu}_g(x,y)\cdot\varepsilon_g(x,y) + \hat{\mu}_l(x,y)\cdot\varepsilon_l(x,y) \quad (1)$$

where $\varepsilon(x)$ is the fraction of contribution of each phase (gas or liquid) in the pixel region $(x,y)$. It is inherent that:

$$\varepsilon_g(x,y) + \varepsilon_l(x,y) = 1 \quad (2)$$

Since $\hat{\mu}_g(x) \ll \hat{\mu}_l(x)$, we can neglect it in Eq. (1), then isolating $\varepsilon_l(x)$ in eq. (1) we have:

$$\varepsilon_g(x,y) = \frac{\hat{\mu}_l(x,y) - \hat{\mu}_{g-l}(x,y)}{\hat{\mu}_l(x,y)} \quad (3)$$

From Eq. (2) it follows that:

$$\varepsilon_l(x,y) = 1 - \varepsilon_g(x,y) = 1 - \frac{\hat{\mu}_l(x,y) - \hat{\mu}_{g-l}(x,y)}{\hat{\mu}_l(x,y)} \quad (4)$$

The reconstructed images (Fig. 2) in terms of holdup ($\varepsilon_g(x,y)$ or $\varepsilon_l(x,y)$), processed from data obtained through CT scans, provide the gas and liquid distributions at $r/R$ axial level, where $r$ is the perimeter region centered around the axis of the column and it varies in the interval of $0 < r \leq R$. $R$ is equal to 40 mm, that is the inner radius of the column. The gas and liquid holdup distributions for bubbles generated in a hole of $\varnothing = 5$ mm, located at 15 mm of the column wall, are shown in Fig. 3. The tomographic measurements were taken at 20 mm, 120 mm and 320 mm height from the bubbles generation center (Fig. 1). At 20 mm, most bubbles are distributed close to the bubble generation center (arrows on the top of Fig. 2). At 120 mm and 320 mm, the images shown in the Fig. 2 do not show the bubble generation center due to a randomized scattering effect of the bubbles. Close to the bubble center, the bubbles are subjected to high pressure due to the 1400 mm water column above them and, in such case, the entropy can be considered lower, while in higher regions from bubble

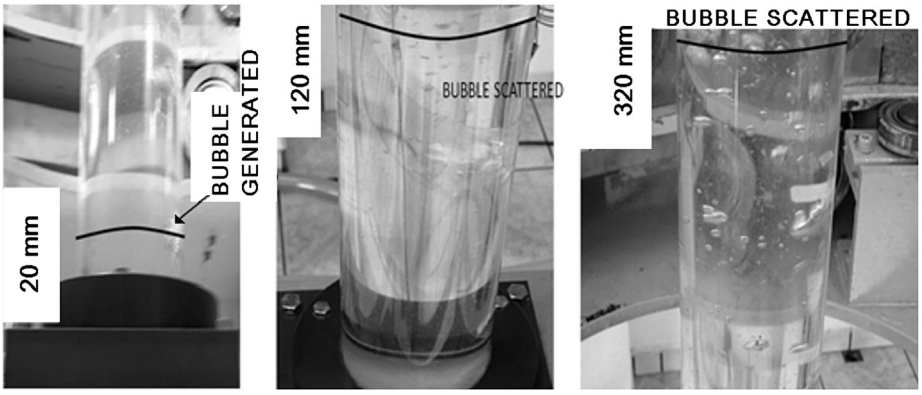


**Fig. 1.** Bubbles scattering along the column height. Tomograms were carried out at 20 mm, 120 mm and 320 mm from the center of air bubble generation. The bubbles are generated using a device containing a hole of $\varnothing = 5$ mm located at 15 mm from the wall column or 25 mm from the geometric center of the column (azimuthal averaging).

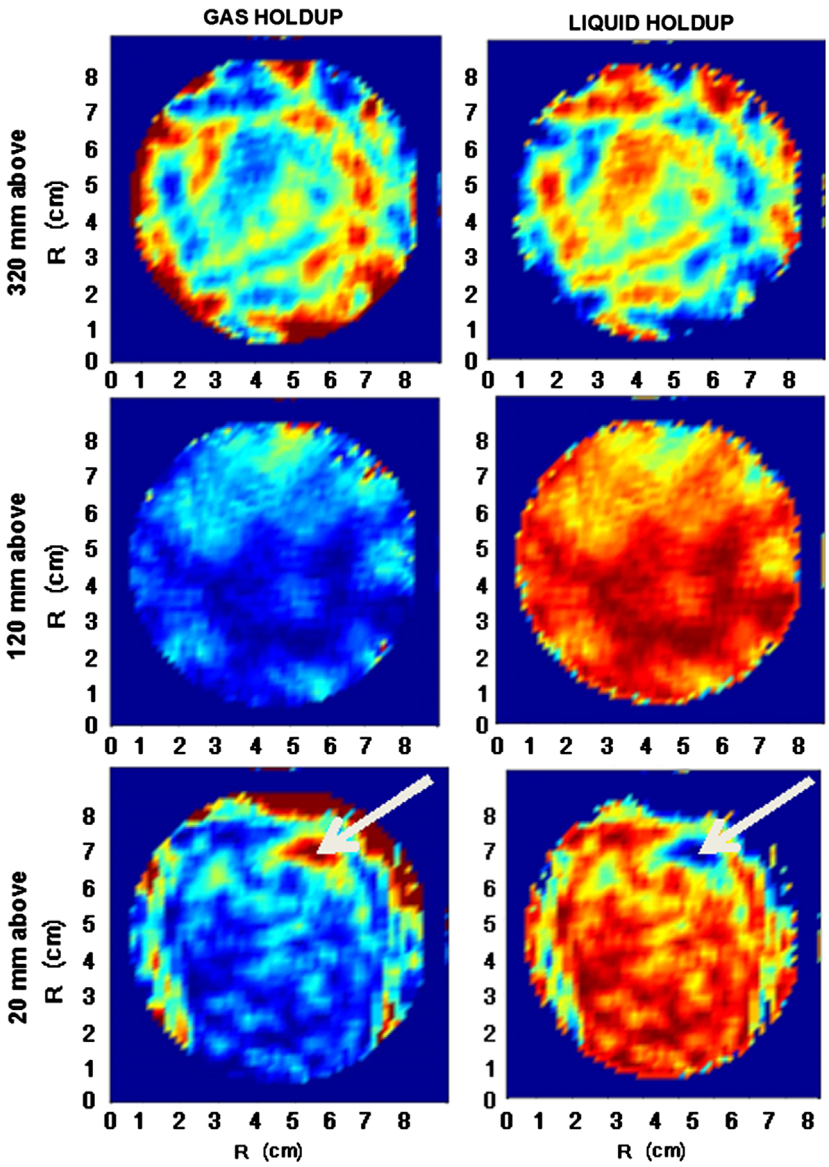


**Fig. 2.** Images generated by AM algorithm from measurements taken at different distances (above 5, 10, 20 and 30 cm from bubble generation center) of a multiphase column (Perspex cylindrical tube of density $\delta \cong 1.2$ g/cm$^3$, $\varnothing_{int}=8$ cm, $\varnothing_{ext}=9$ cm, and 0.5 cm wall thickness). The arrow points to the region of the bubbles generation. The bubbles rise to the top of the column at a speed of about 300 cm/s.

generation center the water pressure decreases; consequently, the bubble volume increases and it can "explode" in new small bubbles and spread out randomly. Such phenomenon involves an entropy burst (Dubnikova et al., 2005), which is the result of formation of new bubbles from the former bubble. These results can be interpreted quantitatively by the analysis shown in Fig. 3. This figure shows, in the $y$ axis, the mean values of $\varepsilon(x,y)$ in concentric rings, at distances $r/R$ $(0 < r \leq R)$. The curves relative to the measurement distances at 20 mm and 320 mm show a peak (gas holdup) and a valley (liquid holdup) at $r/R \cong 0.65$, implying $r = 0.65 \times R (= 40\text{ mm}) \cong 26$ mm, which is the distance from the column center where the concentration of air is higher. Coincidentally, the found value of 26 mm is close to the radial distance from the bubble generation center (actual value of 25 mm). It may be noted that there are two areas that stand out for having the highest concentration of gases, they are: the ring between $r \cong 20$ mm and $r \cong 32$ mm ($0.5 \times R$ and $0.8 \times R$, respectively) and in the column wall $r = R = 40$ mm ($r = 1 \times R = 40$ mm). On the other hand, the CT scan at 120 mm the concentration of gas remained fairly constant all along the radial center of the column, holding up the level of about 2–4% of gas. These considerations can also be inferred from Fig. 1. Observing this figure, in the measurement region of 20 mm, the bubbles are concentrated in the vicinity of the bubble generation center and there is a prevalence of small amounts of bubbles positioned above the bubble generation center which tends to move close to the column wall direction. In the intermediate region of the measurements (at 120 mm) it was observed that bubbles have small size and are randomly distributed with a slight tendency to concentrate near to the tube walls. Finally, in the measurement region of 320 mm the bubbles are subjected to lower water pressure, presenting larger amount of greater bubbles above their generation center and near of the column wall. The bubbles size in the first region (20 mm) and the third region (320 mm) are larger and are more easily detected by CT. On the other hand, in the second region (120 mm) the bubbles have smaller size and the CT may have less sensitivity to detect this bubble population.

The results presented in this study are similar to those described by Youssef et al. (2013), Kong et al. (2012) and Youssef and Al-Dahhan (2009), using two types of scanners: (a) third

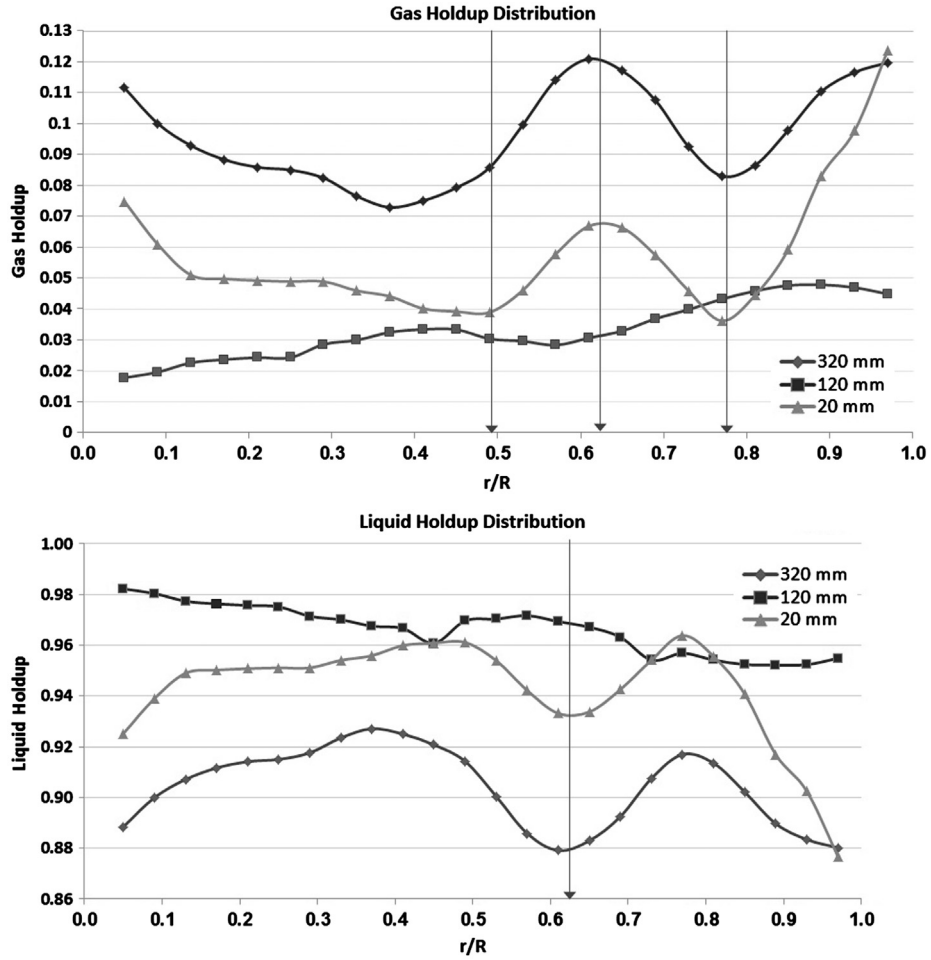


**Fig. 3.** Gas and liquid holdup distributions for bubbles generated in a hole of ∅=5 mm located at 15 mm of the column wall.

generation CT and (b) CARPT (Computer Automated Radioactive Particle Tracking). Also, Johansen (2005) described a fourth generation CT for applications on the multiphase system. Comparatively, the differences in their results are basically the experimental arrangements and the interpretation strategy.

Finally, the main capabilities of the CT to give information about a multiphase process column can be summarized in terms of the reconstructed images and the hold-up curves. The use of a simulation column, where the analyst can visualize directly the phenomena occurring inside the simulation column, leads to the conclusion that the hold-up curves are an important analytical tool. While the reconstructed image allows visualizing the bubble generation center only in a region close to it, the hold-up curves were more efficient to characterize the multiphase column phenomena.

## 4. Conclusions

The third-generation CT was capable of providing composition information of phase (liquid or gas) in two phase systems. Although the system was only capable of providing time-average data, it can provide unique information concerning the structure of two phase systems. Close to the bubble generation center, the bubbles are subjected to high pressure due to the water column above to bubbles and in such case the entropy is lower, while in higher regions of the bubble generation center, the water pressure decreases and the bubble volume increases causing a disruption, dividing it in small bubbles and spread out randomly. This phenomenon involves an entropy burst. The dynamical interaction of bubbles with the column environment (viscosity, pressure and air flow) can cause column regions with different sizes of bubbles that can modify the profile of hold-up curves. For the industrial purpose, the design and scale-up of multiphase flow reactors are of great importance. Any research on the hydrodynamics of such reactors, therefore, needs to enhance the level of understanding of these complex systems and the third generation CT can be a useful tool to give important information of the hydrodynamic processes inside the multiphase systems.

## Acknowledgments

The authors would like to express their gratitude to International Atomic Energy Agency- IAEA and National Council for Scientific and Technological Development (CNPq) for the financial support.

## References

Al-Dahhan, M.H., Kemoun, A., Cartolano, A.R., Roy, S., Dobson, R., Williams, J., 2007. Measuring gas–liquid distribution in a pilot scale monolith reactor via an Industrial Tomography Scanner (ITS). Chem. Eng. J. 130 (2–3), 147–152.

Calvo, W.A.P., Hamada, M.M., Sprenger, F.E., Vasquez, P.A.S., Rela, P.R., Martins, J.F.T., Pereira, J.C.S.M., Omi, N.M., Mesquita, C.H., Vasquez, P.A.S., Carvalho, D.V.S., 2009. Gamma-ray computed tomography scanners for applications in multiphase system columns. Nukleonika 54 (2), 129–133.

Dudukovic, M.P., 2007. Relevance of mutiphase reaction engineering to modern technological challenges. Ind. Eng. Chem. Res. 46, 8674–8686.

Dubnikova, F., Kosloff, R., Almog, J., Zeiri, Y., Boese, R., Itzhaky, H., Alt, A., Keinan, E.J., 2005. Decomposition of triacetone triperoxide is an entropic explosion. Am. Chem. Soc 127 (4), 1146–1159.

Hale, C.P.H., Hu, B., Richardson, S.M., Wong, W.L., 2007. Gammas and X-ray tomography of liquid–liquid and gas–liquid–liquid flows. Multiphase Sci. Technol. 19 (3), 241–267.

Hubbell, J.H., Seltzer, S.M., 1996. Tables of X-ray mass attenuation coefficients and mass energy-absorption coefficients. Nat. Inst. Stand. Technol. (NIST) http://physics.nist.gov/PhysRefData.

International Atomic Energy Agency, Industrial Process Gamma Tomography. IAEA-TECDOC-1589, IAEA, Vienna, 2008.

Johansen, G.A., 2005. Nuclear tomography methods in industry. Nucl. Phys. A 752, 696–705.

Kong, L., Li, Wei, L., Han, L.C., Liu, Y.J., Luo, H., Al Dahhan, M.H., Dudukovic, M.P., 2012. On the measurement of gas holdup distribution near the region of impeller in a gas–liquid stirred Rushton tank by means of γ-CT. Chem. Eng. J. 188, 191–198.

Kumar, S.B., Dudukovic, M.P., 1997. Computer-assisted gamma and X-ray tomography: application to multiphase flow. Proceeding of Non-Invasive Monitoring of Multiphase Flows, Amsterdam, The Netherlands, pp. 48.

Kantarcia, N., Borakb, F., Ulgen, K.O., 2005. Bubble column reactors. Process Biochem. 40, 2263–2283.

Mesquita, C.H.; Vasquez, P.A.S., Calvo, W.A.P., Carvalho, D.V.S., Marcato, L.A., Martins,J.F.T., Hamada, M.M., 2011. Multi-source third-generation computed tomography for industrial multiphase flows applications. in: 2011 IEEE Nuclear Science Symposium Conference Record, 2011, New York, pp. 1294–1302.

Mesquita, C.H., Dantas, C.C., Costa, F.E., Carvalho, D.V.S., Madi Filho, T., Vasquez, P.A. S. Hamada, M.M., 2010. Development of a fourth generation industrial tomography for multiphase systems analysis. in: 2010 IEEE Nuclear Science Symposium Conference Record, 2010, New York, pp. 19–23.

O'Sullivan, J.A., Benac, J., 2007. Alternating minimization algorithms for transmission tomography. IEEE Trans. Med. Imaging 26 (3), 283–297.

Vasquez, P.A.S., Mesquita, C.H., Hamada, M.M., 2010. Methodological analysis of gamma tomography system for large random packed columns. Appl. Radiat. Isot. 68, 658–661.

Wu, Y., Ong, B.C., Al-Dahhan, M.H., 2001. Predictions of radial gas holdup profiles in bubble column reactors. Chem. Eng. Sci. 56, 1207–1210.

Youssef, A.A., Hamed, M.E., Grimes, J.T., Al-Dahhan, M.H., Dudukovic, M.P., 2013. Hydrodynamics of pilot-scale bubble columns: effect of internals. Ind. Eng. Chem. Res. 52, 43–55.

Youssef, A.A., Al-Dahhan, M.H., 2009. Impact of internals on the gas holdup and bubble properties of a bubble column. Ind. Eng. Chem. Res. 48, 8007–8013.